

# Electron Correlation at the $\text{MgF}_2(110)$ Surface: A Comparison of Incremental and Local Correlation Methods

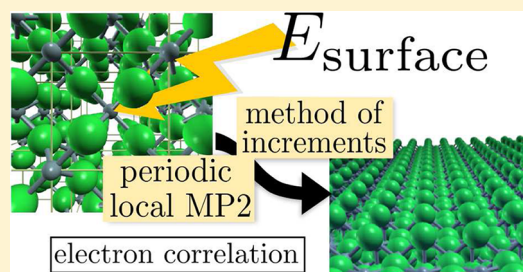
Lukas Hammerschmidt,<sup>\*,†</sup> Lorenzo Maschio,<sup>‡</sup> Carsten Müller,<sup>†</sup> and Beate Paulus<sup>†</sup>

<sup>†</sup>Freie Universität Berlin, Institut für Chemie und Biochemie, Takustr. 3, 14195 Berlin, Germany

<sup>‡</sup>Università di Torino, Dipartimento di Chimica, Via P. Giuria 5, 10125 Torino, Italy

## S Supporting Information

**ABSTRACT:** We have applied the Method of Increments and the periodic Local-MP2 approach to the study of the (110) surface of magnesium fluoride, a system of significant interest in heterogeneous catalysis. After careful assessment of the approximations inherent in both methods, the two schemes, though conceptually different, are shown to yield nearly identical results. This remains true even when analyzed in fine detail through partition of the individual contribution to the total energy. This kind of partitioning also provides thorough insight into the electron correlation effects underlying the surface formation process, which are discussed in detail.



## 1. INTRODUCTION

Magnesium fluoride has been known for its transparency in a broad range of wavelengths for a long time, and thus has been used mainly for the construction of high quality lenses and optical devices. In recent years, the sol–gel synthesis of  $\text{MgF}_2$  as high-surface nanoparticles has aroused interest due to its potential application in heterogeneous catalysis.<sup>1</sup> The shape of such nanoparticles is key in determining their properties as a catalyst and is dictated by the surface formation energy of different cuts of the bulk crystal.<sup>2</sup>

The determination of surface energies is, however, quite a challenging task, both from the experimental and theoretical point of view. Experimentally, surface energies are often obtained by cleavage of planes in a single crystal—not an easy task by itself—and the results are often quite temperature dependent. Consequently, experimental results differ by 10–40% already for simpler systems.<sup>3–6</sup>

From the theoretical side, it is challenging to treat different kinds of interaction, such as ionic, covalent, purely dispersive interactions, at equally high level. The widely adopted density functional theory (DFT) with common functionals is efficient and very often features a reasonable high accuracy.<sup>7,8</sup> However, existing studies indicate that DFT surface energies depend strongly on the applied exchange–correlation functional.<sup>9</sup> This may be due to an insufficient description of the nonlocal electron correlation. For weak interactions, such as physisorption, standard DFT functionals tend to underestimate binding energies.<sup>10–13</sup> The reliability of DFT results has been tremendously improved by the introduction of dispersion corrections, both empirical<sup>14–16</sup> and nonempirical<sup>17,18</sup> ones, as well as nonlocal DFT functionals (e.g., vdW-DF<sup>19</sup> and VV10<sup>20</sup>) and the recent MBD approach by Tkatchenko and co-workers.<sup>21</sup> This, however, is at the price of partly losing the *first principle* character of the method. The most recent

developments beyond DFT, such as doubly hybrid functionals,<sup>22–24</sup> have not been tested on surface energies so far.

Standard implementations of high-level wave function-based electron correlation methods achieve often high accuracies but scale unfavorably with system size.<sup>25</sup> Efficient electron correlation schemes, on the other hand, are often based on localized orbitals and, thus, exploit the local character of the correlation hole. Stollhof and Fulde were among the first ones to introduce the idea of localized orbitals for electron correlation in extended systems later known as the “local ansatz”.<sup>26–28</sup> A slightly amended scheme was developed by Pulay and Saebø,<sup>29–31</sup> which afterward was implemented in the MOLPRO program<sup>32,33</sup> for molecular systems by Werner and Schütz<sup>34–36</sup> and then extended to solids for MP2 by Pisani et al.<sup>37,38</sup> as implemented in the CRYSCOR program.<sup>38,39</sup> The latter implementations are based on an orthogonal set of localized orbitals spanning the occupied manifold, while nonorthogonal projected atomic orbitals (PAOs) are used to represent the virtual space.

A different way of truncating the virtual space for periodic systems was introduced by Stoll via the “method of increments” (MoI).<sup>40–43</sup> The MoI relies on cluster schemes that mimic the infinitely extended system, thus, allowing the application of standard quantum chemistry programs and any implemented, size-extensive method to treat electron correlation through a many body expansion. An automatic incremental scheme for finite systems and embedded clusters is under development.<sup>44</sup> However, cluster schemes are not necessarily the only way to truncate the virtual space in the incremental approach. Shukla et al. applied an incremental scheme that, again, relies on PAOs.<sup>45</sup> Another approach based on clusters is the so-called

Received: September 18, 2014

Published: December 4, 2014

hierarchical method. It is based on an approach by Abdurrahman et al.<sup>46</sup> and was proposed for solids by Manby et al.<sup>47</sup> A more exhaustive overview of developments and applications of correlation methods to the solid state is provided by Müller and Paulus.<sup>25</sup>

The MoI and the periodic Local-MP2 (LMP2) method have both been applied very successfully to describe adsorption energies.<sup>48–55</sup> In this work, we do not only extend both methods to investigate the correlation contribution to surface energies but show that the two approaches are complementary and compare very well. This good comparability allows to exploit the benefits of both methods. One advantage of the method of increments is the applicability of any size consistent electron correlation method, while one advantage of the periodic LMP2 method is the applicability of periodic boundary conditions.

In this work, we predict the surface energy by applying the cluster based method of increments and the periodic LMP2 method. Although both methods are conceptually different, we show that, for the  $\text{MgF}_2$  (110) surface (Figure 1), they

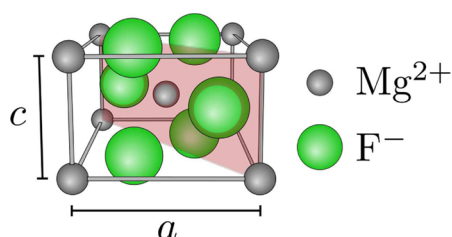


**Figure 1.**  $\text{MgF}_2$  unit cell in the rutile structure. The red, transparent plane indicates the (110) plane. Green (large) circles represent fluorine ions; black (small) circles indicate magnesium ions.  $a$  and  $c$  are the two free lattice parameters.

independently yield surface energy values that are in very good agreement. This agreement allows us to confidently consider both methods to be very accurate. Although we chose  $\text{MgF}_2$  as a test system, our methods are easily adopted to other systems.

As a last remark, we mention that a high-quality, but computationally costly, alternative to the above-mentioned wave function-based electron correlation method is represented by Quantum Monte Carlo (QMC) techniques. Although by definition QMC is exact only for bosons, it is regarded as highly accurate for electronic properties of solids and provides

reasonable surface energies in agreement with quantum chemical methods.<sup>9,56,57</sup>

The paper is structured as follows. In Section 2 we explain the applied methods and other computational details. In Section 3 we discuss our results for the  $\text{MgF}_2$ (110) surface. Conclusions follow in Section 4.

## 2. METHODS

### 2.1. Periodic Local-MP2 Method for Surface Energies.

The local correlation method of Pulay and Saebo<sup>29–31</sup>—which we briefly introduced in Section 1—exploits the exponential decay, with respect to the distance, of Hamilton matrix elements between excited determinants and the ground state determinant by spatially truncating, that is, localizing, the virtual space. A nonorthogonal localized virtual space is achieved by projecting out the occupied space directly from the atomic orbital basis, creating so-called PAOs. Then, the LMP2 correction to the HF wave function is written as<sup>38</sup>

$$|\Psi^{(1)}\rangle = \frac{1}{2} \sum_{(ij) \in P} \sum_{(ab) \in [ij]} T_{ab}^{ij} |\Phi_{ij}^{ab}\rangle \quad (1)$$

where  $\Phi_{ij}^{ab}$  are doubly excited determinants and  $T_{ab}^{ij}$  are the corresponding amplitudes. In eq 1, the labels  $(i, j)$  refer to pairs of occupied Wannier functions (WFs) taken from a truncated list  $P$ , in which the first WF  $i$  is located in the reference unit cell and the second WF  $j$  is restricted within a given distance to the first WF  $i$ . Note that bold indices here combine the index within the unit cell and the translation (lattice) vector:  $\mathbf{i} = i\mathbf{I}$ , in the notation of ref 38. The labels  $(a, b)$  refer to pairs of mutually nonorthogonal virtual PAOs and the sum is restricted to the pair-domain  $[ij]$  of PAOs which are spatially close to at least one of the WF  $i$  or  $j$ . This truncation of the virtual space makes the computational cost of the LMP2 method scale linearly with the supercell size. Relying on the Hartree–Fock (HF) solution and orbital localization of CRYSTAL,<sup>58,59</sup> the method by Pulay and Saebo was adapted for periodic systems by Pisani et al. and implemented into the CRYSCOR program.<sup>38,39</sup>

Constraining the excitation domains often results in practical difficulties, for example, for calculating differences between a system and its constituting parts. For each calculation equally sized excitation domains have to be ensured, otherwise a significant basis set error is introduced. This circumstance prevents a straightforward adaption of the LMP2 calculation to

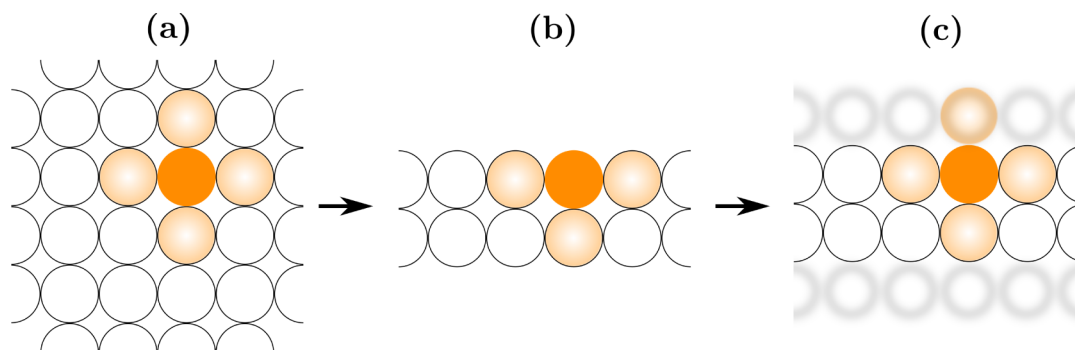


**Figure 2.** Schematic view on a two-dimensional domain construction for a CRYSCOR slab calculation. Dark orange (completely filled) circles represent a center with its light orange (half-filled circles) symbolized excitation domain. A slab is created from a bulk structure (a) by truncating the bulk in one dimension (b), thus truncating the excitation domains. Excitation domain size inconsistencies are circumvented by reintroducing ghost functions (blurry circles) at the former atom positions (c).

relaxed surface energies, as schematically represented in Figure 2. Figure 2a pictorially shows the projection of localized orbitals of a bulk in two dimensions. In this picture, a slab is created by truncating the bulk in one dimension leading to Figure 2b. It is immediately obvious that the truncation in one-dimension leads to a different size of the excitation domain (light orange, half-filled circles) for the center. Maintaining an equal size of the excitation domain can be achieved by introducing ghost atoms in the slab compensating for the missing PAOs (see Figure 2c). The same effect is present as well as BSSE in nonlocal methods but becomes critical within the local approximation due to the severe truncation of the virtual space.

Let us show, in the following, how consistency in the domains can be obtained for surfaces. In general the surface energy,  $E_{\text{surface}}$ , is

$$E_{\text{surface}} = \frac{1}{2A}(E_{\text{slab}} - nE_{\text{bulk}}) \quad (2)$$

where  $E_{\text{slab}}$  is the slab energy per unit cell,  $E_{\text{bulk}}$  the bulk energy per unit cell,  $n$  is the number of formula units in the unit cell of the slab divided by the number of formula units in the bulk unit cell, and  $A$  the surface of the slab unit. Equation 2 can be divided into a HF and a post-HF (i.e., correlation) part

$$2AE_{\text{surface}} = E_{\text{slab}}^{\text{HF}} + E_{\text{slab}}^{\text{corr}} - n(E_{\text{bulk}}^{\text{HF}} + E_{\text{bulk}}^{\text{corr}}) \quad (3)$$

$$E_{\text{surface}} = E_{\text{surface}}^{\text{HF}} + E_{\text{surface}}^{\text{corr}} \quad (4)$$

For an MP2 treatment of the correlation the last term on the right-hand side of eq 4 becomes

$$2AE_{\text{surface}}^{\text{LMP2}} = E_{\text{slab}}^{\text{d4,rlx}} - nE_{\text{bulk}}^{\text{d4}} \quad (5)$$

where  $E_{\text{bulk}}^{\text{d4}}$  is the LMP2 energy of the bulk with an excitation domain for each fluorine that includes 4 ions: the fluorine itself and its three nearest magnesium neighbors (1F, 3Mg).  $E_{\text{slab}}^{\text{d4,rlx}}$  is the LMP2 energy of the relaxed slab with equivalently sized excitation domains as in the bulk. Unfortunately,  $E_{\text{slab}}^{\text{d4,rlx}}$  is not directly accessible, since ghost atoms, which correct for excitation domain sizes, can only be included meaningfully in an unrelaxed slab. In conclusion, eq 5 is rewritten to

$$2AE_{\text{surface}}^{\text{LMP2}} = \Delta E^{\text{rlx}} + E_{\text{slab}}^{\text{d4,unrlx}} - nE_{\text{bulk}}^{\text{d4}} \quad (6)$$

where  $E_{\text{slab}}^{\text{unrlx,d4}}$  is the energy of the unrelaxed slab and  $\Delta E^{\text{rlx}}$  is the relaxation energy. Then, the relaxation energy can be obtained as

$$\Delta E^{\text{rlx}} \approx E_{\text{slab}}^{\text{d3,rlx}} - E_{\text{slab}}^{\text{d3,unrlx}} \quad (7)$$

where d3 indicates a smaller (3-atom) excitation domain for fluorines at the top of the slab—which are missing one of their three nearest neighbors. Thus, the BSSE corrected MP2 surface energy in a CRYSCOR calculation of a relaxed slab is evaluated as

$$E_{\text{surface}}^{\text{MP2}} = \frac{1}{2A}(E_{\text{slab}}^{\text{d4,unrlx}} + E_{\text{slab}}^{\text{d3,rlx}} - E_{\text{slab}}^{\text{d3,unrlx}} - nE_{\text{bulk}}^{\text{d4}}) \quad (8)$$

**2.2. Method of Increments for Surface Energies.** In the method of increments, the correlation energy is expanded in terms of electron correlation contributions (increments) from groups of localized orbitals.<sup>25,40–43</sup> These groups are associated with an atom, an ion, a molecule or a bond between atoms. The total correlation energy,  $E_{\text{corr}}^{\text{solid}}$ , is

$$E_{\text{corr}}^{\text{solid}} = \sum_i \varepsilon_i + \frac{1}{2} \sum_{i \neq j} \Delta \varepsilon_{ij} + \frac{1}{6} \sum_{i \neq j \neq k} \Delta \varepsilon_{ijk} + \dots \quad (9)$$

where  $\varepsilon_i$  is a one-center,  $\Delta \varepsilon_{ij}$  a two-center, and  $\Delta \varepsilon_{ijk}$  a three-center increment.

A one-center increment,  $\varepsilon_i$ , is defined as the electron correlation energy from the electrons in the orbitals of group  $i$ . Here, we consider a group of four orbitals ( $2s^2p^6$ ), of which each group is centered either at a fluorine or a magnesium ion.

The two-center increment,  $\Delta \varepsilon_{ij}$ , considers the nonadditive part of the correlation energy  $\varepsilon_{ij}$  from electrons in the groups  $i$  and  $j$  and is  $\Delta \varepsilon_{ij} = \varepsilon_{ij} - \varepsilon_i - \varepsilon_j$ . Higher order increments are defined accordingly. Since increments decrease rapidly with the order and the intercenter distance, often a small number of one- and two-center increments are enough to obtain more than 97% of the total electron correlation energy.

The method of increments has already been adopted in the study of adsorption energies. In such a calculation, an interaction increment was defined according to the adsorption energy (see, for example, refs 52 and 55). Similar to such an interaction increment, we define a surface increment,  $\sigma$ , which is the difference of an increment in the slab and the corresponding increment in the bulk. Thus, the 1- and 2-body surface increments are defined as

$$\sigma_i = \varepsilon_i^{\text{slab}} - \varepsilon_i^{\text{bulk}} \quad (10)$$

$$\sigma_{ij} = \Delta \varepsilon_{ij}^{\text{slab}} - \Delta \varepsilon_{ij}^{\text{bulk}} \quad (11)$$

where higher order increments are defined accordingly. The index  $i$  runs over all localized orbital groups in the slab unit cell and  $j$  over all other ones that are not necessarily in the same unit cell.  $\varepsilon_i^{\text{bulk}}$  is the  $i$ -th increment in the bulk that corresponds to the  $i$ -th increment in the slab  $\varepsilon_i^{\text{slab}}$ . Corresponding 1-center increments can easily be identified. Identification of corresponding two-center increments is only straightforward for unrelaxed slabs. In this case, the distance between two increments is equal in both structures. For relaxed slabs, distances between centers vary, compared to the bulk. However, also the relaxed slab increments can be assigned to their corresponding equivalent in the unrelaxed slab.

The sum over all surface increments yields the correlation contribution to the surface energy

$$E_{\text{surface}}^{\text{corr}} = \sum_i \omega_i \sigma_i + \sum_{ij} \omega_{ij} \sigma_{ij} + \sum_{ijk} \omega_{ijk} \sigma_{ijk} + \dots \quad (12)$$

where  $\omega$  refers to the weighting factors, that is, how often the specific increment occurs.

In Section 2.1 we show how to calculate the periodic MP2 contribution ensuring an equally sized excitation domain. In the method of increments the effect of domain inconsistencies is partly compensated by considering excitations into the whole virtual space. However, in principle, we can adopt the same BSSE correction of the periodic case to the method of increments. To keep the two methods strictly comparable, we applied the same scheme as in Section 2.1.

### 2.3. Surface Model and Computational Details.

**2.3.1. Structure and Embedding.** The bulk structure that underlies our surface models in the periodic and cluster approach is a rutile-type  $\text{MgF}_2$  structure fully optimized (cell and inner parameters) at the B3LYP level. A detailed investigation of the bulk structure is reported in our previous investigations in refs 55 and 60. We found the cell constants  $a$



and  $c$  and the one free atomic coordinate to be 4.665 Å, 3.083 Å, and 0.304, respectively. The bulk structure was optimized with B3LYP. By definition, incremental post-HF methods do not allow for relaxations based on gradients and up to now no such scheme is implemented in the CRYSCOR code. However, B3LYP optimized lattice parameters of  $\text{MgF}_2$  showed rather good agreement with experimental values in the past.<sup>60</sup> This allows us to confidently calculate relaxations with B3LYP and, afterward, use these structures in a single point MP2 calculation. Consistently, all structure optimizations in the present work, which underlie post-HF computations, have been performed with B3LYP.

Based on the optimized bulk structure, we constructed slabs with 11, 15, 21, and 27 layers with two (110) faces—the most stable low-index surface of  $\text{MgF}_2$ . All four slabs have the same surface termination and contain a mirror plane in the middle of the slab. Due to this symmetry, there are effectively only 5, 8, 11, and 14 layers. Ions were either allowed to relax freely (relaxed slab) or were kept at their bulk positions (unrelaxed slab). For the BSSE correction additional layers of ghost atoms were added on each side of the unrelaxed slab. For the slabs with 5, 8, and 11 layers and the optimized bulk structure we performed single-point periodic HF and periodic LMP2 calculations.

MoI clusters were directly constructed from the relaxed and unrelaxed 11-layered periodic slabs. For each layer individually, a cluster was created with either a fluorine or a magnesium ion in the center. To construct clusters in the middle of the slab, further layers were included and kept at the bulk positions. All clusters consist of at least 45 and at most 57 atoms, depending on the structure. 1-Center increments were always computed for ions that are positioned at the center of the cluster.

Clusters, utilized in the MoI, were embedded in an array of point charges by utilizing the embedding scheme described by Herschend et al.<sup>61</sup> and Müller and Hermansson.<sup>62</sup> The field was constituted by formal point charges of +2 and −1 for magnesium and fluorine ions, respectively, and the field was truncated at a distance of 20 Å from the center of the cluster. Positive point charges next to atoms in the cluster were replaced by Stuttgart effective-core potentials (ECPs)<sup>63</sup> with an effective charge of +2 au.

**2.3.2. Basis Set and Computational Details.** We applied the 8-511d1G basis set by Valenzano et al.<sup>64</sup> for the magnesium ions and the 7-311G basis set by Nada et al.<sup>65</sup> with an additional d-polarization function with an exponent of 0.7 for the fluorine ion. All structure optimizations (slab relaxations) were performed applying DFT and the B3LYP functional as implemented in the CRYSTAL09 program code.<sup>58,59</sup> Shrinking factors of 12 were employed for the Monkhorst–Pack and Gilat k-point net. Values of 8, 8, 8, 20, and 50 were applied as truncation criteria for the bielectronic integrals (cf. CRYSTAL09 manual<sup>59</sup>). An energy convergence criterion of  $10^{-7}$  au was used in the self-consistent field iteration.

Localizations of periodic wave functions were performed for valence electrons only, following the scheme in ref.<sup>66</sup> Default Boys control parameters were applied with initial and final tolerances for the DM matrix element calculation and a convergence criterion of  $10^{-7}$ . In the periodic DF-LMP2, the same shrinking factors as in the HF and DFT calculation were employed for the Monkhorst–Pack and Gilat k-point net. Density fitting was performed purely in direct space using a mixed Gaussian–Poisson auxiliary basis set.<sup>67</sup> Domain sizes have been defined manually to ensure consistency in the LMP2

calculations and were in principle set to 4, including the 3 nearest neighbors of a fluorine and itself (1F, 3Mg). Domains were decreased to 3 atoms (1F, 2Mg) for the relaxed and unrelaxed slab, where fluorine atoms at the surface are explicitly missing one of their coordination partners. Pairs between 0 to 8 Å and 8 to 12 Å were treated as weak and distant, respectively (see ref 39).

Cluster calculations have been performed using the MOLPRO 2012.1 program package.<sup>32,33,68–70</sup> The localization of the canonical Hartree–Fock solution was performed according to the Foster–Boys algorithm.<sup>71</sup> The “active orbitals” were recanonized, for treating the localized orbitals with perturbation methods.

All one-center increments in the unit cells of bulk and slab are included in the many-body expansion as well as pairs of increments with an intercenter distance of smaller than 5 Å. Three-center increments were constructed to consist of centers that are nearest neighbors.

### 3. RESULTS

**3.1. Structure and Slab Convergence.** Surface energies are not only sensitive to structural changes in the slab (relaxation) but also to the number of layers (slab size). This becomes even more important when the aim is to achieve very accurate energies with post-HF methods. Therefore, we selected two criteria to estimate a proper size of our slab model: The first criterion is the convergence of the B3LYP surface energy with slab size; the second criterion is the convergence of the slab relaxation with slab size (measured by the relative shift of the ions in the relaxed slab). In Table 1, we

**Table 1. Surface Energies (in J/m<sup>2</sup>) Calculated with DFT/B3LYP for Unrelaxed and Relaxed Slabs with Different Numbers of Layers<sup>a</sup>**

no. layers	$E_{\text{surface}}^{\text{unrx}}$	$E_{\text{surface}}^{\text{rlx}}$	$\Delta z_i$		
			layer 1, $i = \text{F}$	layer 2, $i = \text{Mg}$	layer 2, $i = \text{F}$
5	0.9207	0.6922	2	73	140
8	0.9202	0.6824	12	109	123
11	0.9201	0.6791	19	117	119
14	0.9199	0.6781	20	118	118

<sup>a</sup>Atom shifts  $\Delta z_i$  (in mÅ) along the  $z$ -axis, between relaxed and unrelaxed slabs, are also reported. These are relative to ions  $i$  in layer 1 and 2 and are evaluated as  $\Delta z_i = z_i^{\text{rlx}} - z_i^{\text{unrx}}$ .

compare surface energies and relative shifts of ions for four relaxed (110) slabs that increase in size and possess equal terminations (see Section 2.3.1). Two main results can be extracted from this data: (i) the surface energy converges fast with the size of the slab, specially in the unrelaxed case; (ii) the structural relaxation converges less quickly. Based on these results, we chose the 11-layer slab for all post-HF computations. This slab is converged in surface energy and structural relaxation to values smaller than 1 mJ/m<sup>2</sup> and 2 mÅ, respectively.

We assess the BSSE with three methods, the HF, the B3LYP and the LMP2 method, by calculating the surface energy,  $E_{\text{surface}}$  (see Table 2).  $E_{\text{surface}}^{\text{HF}}$ ,  $E_{\text{surface}}^{\text{B3LYP}}$ , and  $E_{\text{surface}}^{\text{LMP2}}$  converge nicely after two layers of ghost atoms with an accuracy as high as 1 mJ/m<sup>2</sup> or higher. Thus, we include two layers of ghost functions in all calculations that consider BSSE corrections. The effect of BSSE

**Table 2.** Surface Energies (in J/m<sup>2</sup>) Calculated with DFT/B3LYP, HF, or LMP2 for Unrelaxed Slabs with Additional Numbers of Ghost Layers<sup>a</sup>

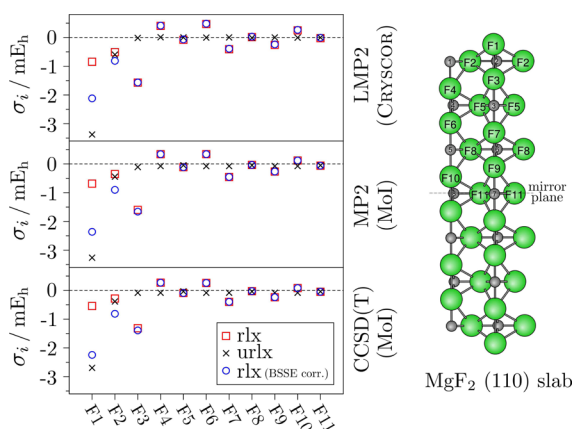
no. ghost layers	$E_{\text{surface}}^{\text{B3LYP}}$	$E_{\text{surface}}^{\text{HF}}$	$E_{\text{surface}}^{\text{MP2}}$
0	0.9201	0.9754	0.9741
1	0.8692	0.9453	0.9285
2	0.8339	0.9215	0.8735
3	0.8337	0.9206	0.8744
4	0.8336	0.9205	0.8743

<sup>a</sup>A ghost layer is a layer of atoms, where the atoms have been replaced by their corresponding basis sets.

corrections on the MgF<sub>2</sub>(110) surface energy for various methods is shown in the Supporting Information.

**3.2. Electron Correlation in the Surface.** One of the great advantages of local correlation methods is the possibility to partition electron correlation contribution spatially. This allows to examine electron correlation in a very detailed picture. One point is, for example, how the correlation energy emerges when approaching a bulk like layer starting from a surface layer. Expectations are that an increment deep in the slab is very similar to an increment in the bulk. To verify this assumption, in the MoI we simply analyze the 1-body surface increments  $\sigma_i$ . An equivalent 1-body increment can also be defined in the periodic LMP2 method, by summing over all MP2 energy pairs that arise solely from a certain ion (center).

Upon approaching lower layers,  $\sigma_i$  is expected to converge to zero. Indeed, such a behavior is observed for both, relaxed and unrelaxed, slabs (cf. Figure 3). However, only in the unrelaxed

**Figure 3.** Surface increments ( $\sigma_i = \epsilon_i^{\text{slab}} - \epsilon_i^{\text{bulk}}$ ) for fluorine ions from F1 to F11. Results are presented for relaxed (rlx, red cubes), unrelaxed (urlx, black crosses), and excitation domain consistent (rlx BSSE corr., blue circles) slab calculations.

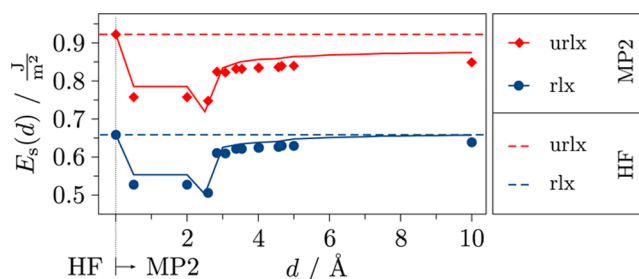
structure  $\sigma_i$  converges monotonically already in the third layer. The convergence is not monotonic anymore in the relaxed case. Upon relaxation the former large electron correlation energy difference at the surface is smeared out over the whole slab. Convergence, although it is achieved, is only reached for the deepest layers.

All three methods independently result qualitatively in the same convergence behavior; for all methods surface increments converge equally. The largest differences appear between CCSD(T) and MP2 surface increments, although these differences are small. In conclusion, surface increments are already surprisingly well described by MP2. Between MP2 in

the MoI and the periodic LMP2 the agreement is excellent. This means that (i) embedding errors in the MoI are negligible and (ii) excitation domains in periodic LMP2 are sufficiently large. Both points name the two largest error sources when directly comparing both approaches.

An illustrative analysis, as given before, is not possible for all 2-body surface increments individually: there are simply too many of them. However, we can evaluate the contribution of the two-center surface increments by partitioning them according to their intercenter distances  $d$ . In the same way, we can also partition pair energies in periodic LMP2. In that case, the distance  $d$  refers not to the centers (ions) but to the centroids of the localized Wannier functions. However, for both methods such a partitioning sums up all MP2 energy contributions (including 1-body contributions) up to a distance  $d$  and this allows us again to compare between both methods.

Starting from the HF level, the aforementioned partitioning is shown in Figure 4. Apart from a shift by the relaxation energy

**Figure 4.** Surface energy,  $E_{\text{surface}}$ , including the sum of MP2 pair energy contributions up to a pair distance  $d$ . For MoI,  $d$  is the distance between two increments, that is, ions. In the case of periodic LMP2, the distance  $d$  refers to centers of Wannier functions (see ref 39). Symbols indicate MP2 values obtained with MoI. Solid lines refer to periodic LMP2 values. For periodic LMP2  $d$  was increased by steps of 0.5 Å. The MoI distances are the actual nearest neighbor distances of two centers in the unrelaxed structure. Incremental results for  $d = 10$  Å are extrapolated from periodic LMP2.

the relaxed and unrelaxed profiles are similar. A first, remarkable result is that the periodic LMP2 and MoI compare again excellently. The agreement weakens when we correct for BSSE errors: the BSSE is less pronounced in the periodic-LMP2, mostly due to the truncation of the excitation domains. The excellent agreement allows us to confidently extrapolate our incremental expansion with the LMP2 result to larger pair distances. An extrapolated value for 10 Å is given in Figure 4.

The partitioning reveals that short-range correlation up to  $d \leq 2.585$  Å favors and stabilizes the slab, that is, reduces the surface energy. This can be understood in general terms by thinking that electrons on the surface are more “free” to move and can avoid each other more efficiently than in the bulk. At the same time, long-range correlation with  $d > 2.6$  Å favors the bulk and destabilizes the slab, that is, increases the surface energy.

A detailed explanation for these results can be found on an incremental level. A surface increment in the MoI is the (incremental) correlation contribution to the surface energy. Hence, electron correlation contributions to the surface energy can be classified as stabilizing or destabilizing. This allows to extract some general trends (a detailed list of sums of increments is given in the Supporting Information). The first three 1-body surface increments at the top of the slab favor the

surface. Increments deeper in the slab contribute much less and in the relaxed surface their contributions can also be destabilizing. However, the sum of all 1-body increments still favors the slab.

Besides the composing centers and their intercenter distance, contributions of two-center surface increments,  $\sigma_{ij}$ , are mostly dominated by the appearance or absence of individual 2-body increments,  $\Delta\epsilon_{ij}$ , in the 3D or 2D system, respectively. Upon formation of a slab, ions at the surface loose coordination partners. As a consequence, some 2-body increments, that originally appear in the bulk, are missing in the slab ( $\Delta\epsilon_{ij}^{\text{slab}} = 0$ ). In such a case, eq 11 simply reduces to  $\sigma_{ij} = \sigma_{ij}^b = -\Delta\epsilon_{ij}^{\text{bulk}}$  and since increments are negative ( $\Delta\epsilon_{ij}^{\text{bulk}} < 0$ ) these correlation contributions destabilize the surface. Additionally, these  $\sigma_{ij}^b$  surface increments are always large and contribute significantly.

$\sigma_{ij}^b$  increments appear for the first time in the group of 2-body increments with  $d = 2.841$  Å. Consequently, the destabilizing correlation contribution, that arises from the sum of this group, constitutes the largest amount of 2-body electron correlation to the surface energy. There are no  $\sigma_{ij}^b$  for surface increments with  $d = 2.585$  Å,  $d = 3.083$  Å, and  $d = 4.024$  Å. As a consequence, these groups of increments stabilize, i.e. favor, the surface and their contribution is small.  $\sigma_{ij}^b$  increments occur again in all other groups of 2-body surface increments. However, their contribution is also minor, due to their already large spatial separation. The same discussion as above could be carried out using the periodic-LMP2 terminology, with identical conclusions.

**3.3. Surface Energy.** Kulifeev et al. are the only ones who published experimentally determined surface energies for  $\text{MgF}_2$  so far.<sup>72</sup> Unfortunately, a comparison to our results is impossible. Kulifeev et al. based their estimations on the rising drop method at temperatures close to the melting point. Thus, such a surface energy is by definition only exact at high temperatures and for isotropic solids. Despite these deficiencies, we believe Kulifeev's experimental value should be mentioned, rather for completeness than as a reference value. Kulifeev et al. estimate a surface energy of  $0.24 \text{ J/m}^2$ .

Our computationally obtained surface energies are summarized in Table 3. Consistently, all methods reveal a relaxation energy  $\Delta E_{\text{surface}}$  in the range of  $0.2 \text{ J/m}^2$ ; the effect of including dispersion effects, either empirically by -D3 corrections or through MP2, is to reduce the value of  $\Delta E_{\text{surface}}$ . Concerning surface energies, hybrid and GGA functionals predict values that are in very good agreement with each other. The only exceptions are LDA and the dispersion corrected functionals. LDA, PBE-D3 and B3LYP-D3 result in surface energies that are about 30% larger than predicted with GGA and hybrid functionals.

The HF surface energy is generally larger than GGA and hybrid functionals but still smaller than LDA or DFT-D3 surface energies. Regardless of the method, the total electron correlation contribution to the surface energy is small. As discussed earlier, the individual electron correlation contributions are much larger but short- and long-range contributions cancel each other almost completely. As a consequence, HF already describes the surface energy surprisingly well.

Between the canonical MP2 as employed in the MoI and the periodic LMP2 the agreement is again very good (see bottom of Table 3). The agreement is even better if we compare periodic LMP2 to the extrapolated MP2 value in the MoI (labeled in Table 3 as ext. pol.). From the extrapolated value we can also estimate the error introduced by the spatial truncation

**Table 3. Surface Energies,  $E_{\text{surface}}$  (in  $\text{J/m}^2$ ), for Various Standard DFT Functionals, the LMP2 Method as Implemented in CRYSCOR<sup>38,39</sup> and Canonical MP2 and CCSD(T) as Employed via the Method of Increments (MoI)<sup>a</sup>s**

			$E_{\text{surface}} \text{ (J/m}^2\text{)}$		$\Delta E_{\text{surface}} \text{ (J/m}^2\text{)}$	
method			rlx	unrlx		
periodic	DFT	LDA	0.792	0.980	−0.188	
		PBE	0.569	0.809	−0.240	
		PBE-D3	0.780	0.976	−0.196	
		PW91	0.576	0.810	−0.234	
		B3PW	0.565	0.799	−0.234	
		B3LYP	0.593	0.834	−0.241	
		B3LYP-D3	0.958	1.180	−0.222	
		HF	0.642	0.894	−0.252	
		HF (ref.)	0.658	0.922	−0.264	
		cluster	CRYSCOR	LMP2	0.657	0.874
MoI	MP2			0.629	0.837	−0.208
	MP2 (ext. pol.)			0.638	0.846	−0.208
	MP2+c			0.650	0.858	−0.208
	CCSD(T)			0.651	0.861	−0.210
	CCSD(T)+c			0.681	0.882	−0.201

<sup>a</sup>In the case of MoI “+c” indicates inclusion of electron correlation of the 2s2p shell of  $\text{Mg}^{2+}$  ions. In the case of HF “ref.” indicates the reference for post-HF calculations. All surface energies are BSSE corrected. The relaxation energy,  $\Delta E_{\text{surface}}$ , is finally reported as the difference between the two preceding columns.

of the incremental expansion, that is about  $0.01 \text{ J/m}^2$ . As already stated in Section 3.2, the remaining differences can have two main sources. One of them is the truncation in the excitation space inherent in the local approach, the other one is the cluster approximation in the incremental calculations. However, these errors are small and of the size of  $0.02 \text{ J/m}^2$ .

CCSD(T) surface energies are very close to MP2 energies. MP2 underestimates the surface energy by about  $0.022 \text{ J/m}^2$ , compared to CCSD(T). Thus, already MP2 includes most of the  $\text{MgF}_2$  (110) electron correlation in the surface energy.

From the method of increments we can also estimate the correlation contribution from the 2s2p electrons of the Mg ions. Sometimes this contribution is referred to as core correlation. In some cases, such a core correlation can contribute significantly. In our case, the core correlation is very small, due to canceling incremental contributions, and about  $0.02 \text{ J/m}^2$  and  $0.03 \text{ J/m}^2$  for MP2 and CCSD(T), respectively.

Throughout our study we showed the excellent comparability from both periodic LMP2 and MoI. However, from a computational point of view both methods require very different user efforts. While the periodic LMP2 method allows in principle a very straightforward mostly automated way of calculating the MP2 energy and is, therefore, quite fast, the MoI requires the user to carefully create and embed clusters individually. However, this allows to directly apply any size extensive method and once the clusters are selected the following calculations can be run in parallel. A parallel implementation of the periodic LMP2 in CRYSCOR is under development and will increase the applicability of the method to even larger systems.<sup>73</sup>



## 4. CONCLUSION

Although MoI and periodic LMP2 are based either on clusters or periodic boundary conditions, they both perform very well and are in excellent agreement. The mutual local character of both methods allows to analyze the surface electron correlation in great detail.

Mainly two competitive effects determine whether the total electron correlation contribution favors or opposes the formation of a surface. On the one side, electrons at the surface gain additional “freedom” to move and avoid each other more effectively. On the other side, surface ions lose their coordination partners and thus lose correlation energy from the binding. The first effect is of a rather short-range character, the second effect is more long-ranged, which is reflected by the one- and two-center contributions, respectively.

While standard DFT generally underestimates the  $\text{MgF}_2$  (110) surface energy, LDA, and DFT-D3 being the exception to the contrary, HF lies already very close to the post-HF results. Surface energies are 0.66, 0.65, and  $0.68 \text{ J/m}^2$  for periodic LMP2 (without Mg 2s2p correlation), MP2 (MoI), and CCSD(T) (MoI), respectively.

## ■ ASSOCIATED CONTENT

### Supporting Information

This material is available free of charge via the Internet at <http://pubs.acs.org/>.

## ■ AUTHOR INFORMATION

### Corresponding Author

\*E-mail: luk.hamm@fu-berlin.de. Phone: +49 (0)30 83853745. Fax: +49 (0)30 83854792.

### Notes

The authors declare no competing financial interest.

## ■ ACKNOWLEDGMENTS

This project was supported by the Zentraleinrichtung für Datenverarbeitung (ZEDAT) at the Freie Universität Berlin. We gratefully acknowledge financial support by the Deutsche Forschungsgemeinschaft (Graduate School 1582 “Fluorine as key element”). L.H. gratefully acknowledges travel funds by the International Max Planck Research School “Complex Surfaces in Material Science”.

## ■ REFERENCES

- (1) Rudiger, S.; Kemnitz, E. *Dalton Trans.* **2008**, 1117–1127.
- (2) Kanaki, E.; Gohr, S.; Müller, C.; Paulus, B. *Surf. Sci.* **2015**, 632, 158–163.
- (3) Gilman, J. J. *J. Appl. Phys.* **1960**, 31, 2208–2218.
- (4) Gutshall, P. L.; Gross, G. E. *J. Appl. Phys.* **1965**, 36, 2459–2460.
- (5) Kraatz, P.; Zoltai, T. *J. Appl. Phys.* **1974**, 45, 4741–4750.
- (6) Burns, S. J.; Webb, W. W. *J. Appl. Phys.* **1970**, 41, 2086–2095.
- (7) Kohn, W.; Sham, L. J. *Phys. Rev.* **1965**, 140, A1133–A1138.
- (8) Hohenberg, P.; Kohn, W. *Phys. Rev.* **1964**, 136, B864–B871.
- (9) Binnie, S.; Sola, E.; Alfè, D.; Gillan, M. *Mol. Simul.* **2009**, 35, 609–612.
- (10) Krityán, S.; Pulay, P. *Chem. Phys. Lett.* **1994**, 229, 175–180.
- (11) Hobza, P.; Sponer, J.; Reschel, T. *J. Comput. Chem.* **1995**, 16, 1315–1325.
- (12) Pérez-Jordá, J. M.; Becke, A. D. *Chem. Phys. Lett.* **1995**, 233, 134–137.
- (13) Pérez-Jordá, J. M.; San-Fabián, E.; Pérez-Jiménez, A. J. *J. Chem. Phys.* **1999**, 110, 1916–1920.
- (14) Grimme, S. *J. Comput. Chem.* **2006**, 27, 1787–1799.
- (15) Grimme, S.; Antony, J.; Ehrlich, S.; Krieg, H. *J. Chem. Phys.* **2010**, 132, 154104.
- (16) Civalleri, B.; Zicovich-Wilson, C.; Valenzano, L.; Ugliengo, P. *CrystEngComm* **2008**, 10, 405–410.
- (17) de-la Roza, A. O.; Johnson, E. R. *J. Chem. Phys.* **2012**, 137, 054103.
- (18) Tkatchenko, A.; Scheffler, M. *Phys. Rev. Lett.* **2009**, 102, 073005.
- (19) Dion, M.; Rydberg, H.; Schröder, E.; Langreth, D. C.; Lundqvist, B. I. *Phys. Rev. Lett.* **2004**, 92, 246401.
- (20) Vydrov, O. A.; Van Voorhis, T. *J. Chem. Phys.* **2010**, 133, 244103.
- (21) Schatschneider, B.; Liang, J.; Reilly, A. M.; Marom, N.; Zhang, G. X.; Tkatchenko, A. *Phys. Rev. B* **2013**, 87, 060104.
- (22) Grimme, S. *J. Chem. Phys.* **2006**, 124, 034108.
- (23) Sharkas, K.; Toulouse, J.; Savin, A. *J. Chem. Phys.* **2011**, 134, 064113.
- (24) Sharkas, K.; Toulouse, J.; Maschio, L.; Civalleri, B. *J. Chem. Phys.* **2014**, 141, 044105.
- (25) Müller, C.; Paulus, B. *Phys. Chem. Chem. Phys.* **2012**, 14, 7605–7614.
- (26) Stollhoff, G.; Fulde, P. *Z. Phys. B* **1977**, 26, 257–262.
- (27) Stollhoff, G.; Fulde, P. *J. Chem. Phys.* **1980**, 73, 4548–4561.
- (28) Stollhoff, G. *J. Chem. Phys.* **1996**, 105, 227–234.
- (29) Pulay, P. *Chem. Phys. Lett.* **1983**, 100, 151–154.
- (30) Pulay, P.; Saebo, S. *Theoret. Chim. Acta* **1986**, 69, 357–368.
- (31) Saebo, S.; Pulay, P. *J. Chem. Phys.* **1987**, 86, 914–921.
- (32) Werner, H.-J. et al. MOLPRO, version 2012.1, a package of ab initio programs. 2012; see <http://www.molpro.net> (accessed Nov. 28, 2014).
- (33) Werner, H.-J.; Knowles, P. J.; Knizia, G.; Manby, F. R.; Schütz, M. *WIREs Comput. Mol. Sci.* **2012**, 2, 242–253.
- (34) Hampel, C.; Werner, H.-J. *J. Chem. Phys.* **1996**, 104, 6286–6297.
- (35) Schütz, M.; Hetzer, G.; Werner, H.-J. *J. Chem. Phys.* **1999**, 111, 5691–5705.
- (36) Schütz, M.; Hetzer, G.; Werner, H.-J. *Phys. Chem. Chem. Phys.* **2002**, 4, 3941–3947.
- (37) Pisani, C.; Busso, M.; Capecchi, G.; Casassa, S.; Dovesi, R.; Maschio, L.; Zicovich-Wilson, C.; Schütz, M. *J. Chem. Phys.* **2005**, 122, 094113.
- (38) Pisani, C.; Maschio, L.; Casassa, S.; Halo, M.; Schütz, M.; Usvyat, D. *J. Comput. Chem.* **2008**, 29, 2113–2124.
- (39) Pisani, C.; Schütz, M.; Casassa, S.; Usvyat, D.; Maschio, L.; Lorenz, M.; Erba, A. Cryscor: a program for the post-Hartree-Fock treatment of periodic systems. *Phys. Chem. Chem. Phys.* **2012**, 14, 7615.
- (40) Stoll, H. *Chem. Phys. Lett.* **1992**, 191, 548–552.
- (41) Stoll, H. *J. Chem. Phys.* **1992**, 97, 8449–8454.
- (42) Stoll, H. *Phys. Rev. B* **1992**, 46, 6700–6704.
- (43) Paulus, B. *Phys. Rep.* **2006**, 428, 1–52.
- (44) Friedrich, J.; Hanrath, M.; Dolg, M. *J. Chem. Phys.* **2007**, 126, 154110.
- (45) Shukla, A.; Dolg, M.; Fulde, P.; Stoll, H. *Phys. Rev. B* **1999**, 60, 5211–5216.
- (46) Abdurahman, A.; Shukla, A.; Dolg, M. *J. Chem. Phys.* **2000**, 112, 4801–4805.
- (47) Manby, F. R.; Alfe, D.; Gillan, M. J. *Phys. Chem. Chem. Phys.* **2006**, 8, 5178–5180.
- (48) Martinez-Casado, R.; Mallia, G.; Usvyat, D.; Maschio, L.; Cassassa, S.; Schütz, M.; Harrison, N. M. *J. Chem. Phys.* **2011**, 134, 014706.
- (49) Halo, M.; Cassassa, S.; Maschio, L.; Pisani, C.; Dovesi, R.; Ehinon, D.; Baraille, I.; Rérat, M.; Usvyat, D. *Phys. Chem. Chem. Phys.* **2011**, 13, 4434–4443.
- (50) Usvyat, D.; Sadeghian, K.; Maschio, L.; Schütz, M. *Phys. Rev. B* **2012**, 86, 045412.
- (51) Müller, C.; Paulus, B.; Hermansson, K. *Surf. Sci.* **2009**, 603, 2619–2623.
- (52) Müller, C.; Herschend, B.; Hermansson, K.; Paulus, B. *J. Chem. Phys.* **2008**, 128, 214701.

- (53) Müller, C.; Hermansson, K.; Paulus, B. *Chem. Phys.* **2009**, *362*, 91–96.
- (54) Staemmler, V. *J. Phys. Chem. A* **2011**, *115*, 7153–7160.
- (55) Hammerschmidt, L.; Müller, C.; Paulus, B. *J. Chem. Phys.* **2012**, *136*, 124117.
- (56) Alfè, D.; Gillan, M. J. *J. Phys.: Condens. Matter* **2006**, *18*, L435.
- (57) Binnie, S. J.; Nolan, S. J.; Drummond, N. D.; Alfè, D.; Allan, N. L.; Manby, F. R.; Gillan, M. J. *Phys. Rev. B* **2010**, *82*, 165431.
- (58) Dovesi, R.; Orlando, R.; Erba, A.; Zicovich-Wilson, C. M.; Civalieri, B.; Casassa, S.; Maschio, L.; Ferrabone, M.; De La Pierre, M.; D'Arco, P.; Noel, Y.; Causa, M.; Rerat, M.; Kirtman, B. *Int. J. Quantum Chem.* **2014**, *114*, 1287.
- (59) Dovesi, R.; Saunders, V. R.; Roetti, C.; Orlando, R.; Zicovich-Wilson, C. M.; Pascale, F.; Civalieri, B.; Doll, K.; Harrison, N. M.; Bush, I. J.; D'Arco, P.; Llunell, M.; Causa, M.; Noel, Y. *CRYSTAL14 User's Manual*; University of Torino: Torino, 2014.
- (60) Hüsages, Z.; Müller, C.; Paulus, B.; Hough, C.; Harrison, N.; Kemnitz, E. *Surf. Sci.* **2013**, *609*, 73–77.
- (61) Herschend, B.; Baudin, M.; Hermansson, K. *J. Chem. Phys.* **2004**, *120*, 4939–4948.
- (62) Müller, C.; Hermansson, K. *Surf. Sci.* **2009**, *603*, 3329–3338.
- (63) Fuentealba, P.; von Szentpály, L.; Preuss, H.; Stoll, H. *J. Phys. B* **1985**, *18*, 1287–1296.
- (64) Valenzano, L.; Noël, Y.; Orlando, R.; Zicovich-Wilson, C. M.; Ferrero, M.; Dovesi, R. *Theor. Chem. Acc.* **2007**, *117*, 991–1000.
- (65) Nada, R.; Catlow, C. R. A.; Pisani, C.; Orlando, R. *Modelling Simul. Mater. Sci. Eng.* **1993**, *1*, 165–187.
- (66) Zicovich-Wilson, C. M.; Dovesi, R.; Saunders, V. R. *J. Chem. Phys.* **2001**, *115*, 9708–9719.
- (67) Schütz, M.; Usvyat, D.; Lorenz, M.; Pisani, C.; Maschio, L.; Casassa, S.; Halo, M. *Condensed-Phase Quantum Chemistry, Series: Computation in Chemistry*; CRC Press: Boca Raton, FL, 2010; Vol. 27.
- (68) Hampel, C.; Peterson, K.; Werner, H.-J. *Chem. Phys. Lett.* **1992**, *190*, 1–12.
- (69) Werner, H.-J.; Knowles, P. J. *J. Chem. Phys.* **1985**, *82*, 5053–5063.
- (70) Knowles, P. J.; Werner, H.-J. *Chem. Phys. Lett.* **1985**, *115*, 259–267.
- (71) Boys, S. F. *Rev. Mod. Phys.* **1960**, *32*, 296–299.
- (72) Kulifeev, V. K.; Panchishnyi, V. I. *Izvestiya Vysshikh Uchebnykh Zavednij - Tsvetnaya Metallurgiya* **1969**, *12* (1), 80–82.
- (73) Maschio, L. Local MP2 with Density Fitting for Periodic Systems: A Parallel Implementation. *J. Chem. Theory Comput.* **2011**, *7* (9), 2818–2830.